Biochemical and Biophysical Research Communications 395 (2010) 168–172

Contents lists available at ScienceDirect

Biochemical and Biophysical Research Communications

journal homepage: www.elsevier.com/locate/ybbrc

# The prostaglandin transporter PGT transports $PGH_2$

Yuling Chi [a], Victor L. Schuster [a,b,*]

[a] Department of Medicine, Division of Nephrology, Albert Einstein College of Medicine, Bronx, NY 10461, USA
[b] Department of Physiology and Biophysics, Albert Einstein College of Medicine, Bronx, NY, USA

ARTICLE INFO

*Article history:*
Received 8 March 2010
Available online 25 March 2010

*Keywords:*
Prostaglandin $H_2$
Prostaglandin transporter
Kinetics

ABSTRACT

Prostaglandin $H_2$ not only serves as the common precursor of all other PGs, but also directly triggers signals (e.g. platelet aggregation), depending on its location and translocation. The prostaglandin carrier PGT mediates the transport of several prostanoids, such as $PGE_2$, and $PGF_{2\alpha}$. Here we used PGT in the plasma membrane as a model system to test the hypothesis that PGT also transports $PGH_2$. Using wild-type and PGT-expressing MDCK cells, we show that $PGH_2$ uptake is mediated both by simple diffusion and by PGT. The $PGH_2$ influx permeability coefficient for diffusion is $(5.66 \pm 0.63) \times 10^{-6}$ cm/s. The kinetic parameters of $PGH_2$ transport by PGT are $K_m = 376 \pm 34$ nM and $V_{max} = 210.2 \pm 11.4$ fmol/mg protein/s. $PGH_2$ transport by PGT can be inhibited by excess $PGE_2$ or by a PGT inhibitor. We conclude that PGT may play a role in transporting $PGH_2$ across cellular membranes.

© 2010 Elsevier Inc. All rights reserved.

## 1. Introduction

Prostaglandin $H_2$ ($PGH_2$) is the common precursor of all other PGs ($PGE_2$, $PGI_2$, $PGD_2$, and $PGF_{2\alpha}$) and thromboxane $A_2$ ($TxA_2$). It is converted to these PGs by the specific terminal synthases in the cytoplasm [1–6]. Besides serving as a common precursor, extracellular $PGH_2$ can directly trigger signals including $Ca^{2+}$ release, serotonin release, vasoconstriction, and platelet aggregation [7–10]. The signals induced by extracellular $PGH_2$ can therefore oppose the signals resulting from intracellular $PGH_2$, such as formation of $PGI_2$, the most potent endogenous inhibitor of platelet aggregation [11,12]. Thus the net result of $PGH_2$ depends on its localization. Of interest, Kent et al. [9] reported that endothelial cells exposed to $PGH_2$ produced $PGI_2$, suggesting that $PGH_2$ might be taken up into endothelial cells and converted to $PGI_2$ by $PGI_2$ synthase. This raises the question of how $PGH_2$ translocation occurs.

The prostaglandin transporter (PGT) has been shown to transport several prostaglandins, including $PGE_2$ [13,14]. PGT mediates the active uptake of $PGE_2$ into the cell against a concentration gradient [15]. Based on the structural similarity between $PGH_2$ and $PGE_2$, as shown in Fig. 2C and D, we hypothesized that PGT might also transport $PGH_2$. Using MDCK cells stably expressing PGT, as previously reported [16], we conducted a detailed investigation of the kinetics of $PGH_2$ transport by PGT. The competition of transport by PGT between $PGH_2$ and $PGE_2$, and the inhibition of $PGH_2$ transport by our newly identified PGT inhibitor, TGBz T34 [15], confirmed that $PGH_2$ is, indeed, a substrate of PGT.

## 2. Materials and methods

MDCK cells were stably transfected with the GFP-tagged PGT in our laboratory [16]. Tritium labeled $PGE_2$ ($[^3H]PGE_2$) and $PGH_2$ ($[^3H]PGH_2$) were purchased from PerkinElmer and CaymanChem, respectively. Unlabeled $PGE_2$ was obtained from CaymanChem.

### 2.1. Time course of $PGH_2$ or $PGE_2$ transport

MDCK cells were seeded at 15–20% confluence on 24-well plates. The day on which the cells were seeded was considered day one. $PGE_2$ uptake experiments were conducted on day 4. All of the $PGH_2$ or $PGE_2$ uptake experiments were conducted at room temperature. On day 4, cells were washed twice with Waymouth buffer (135 mM NaCl, 13 mM H–Hepes, 13 mM Na–Hepes, 2.5 mM $CaCl_2$, 1.2 mM $MgCl_2$, 0.8 mM $MgSO_4$, 5 mM KCl, and 28 mM D-glucose). Then 200 μL of Waymouth buffer containing 1 μM $[^3H]PGH_2$ or 1 nM $[^3H]PGE_2$ were added to each well. At the designated time, the uptake of $[^3H]PGH_2$ or $[^3H]PGE_2$ was stopped by aspiration of uptake buffer, followed immediately by two washes with 500 μL of chilled Waymouth buffer. Cells were then lysed with 100 μL lysis buffer containing 0.25% SDS and 0.05 N NaOH. 1.5 mL of scintillation solution was added to each

*Abbreviations:* PG, prostaglandin; PGT, prostaglandin transporter; $PGH_2$, prostaglandin $H_2$; $PGE_2$, prostaglandin $E_2$; AA, arachidonic acid; $TxA_2$, thromboxane $A_2$; COX, cyclooxygenase; ER, endoplasmic reticulum

* Corresponding author at: Department of Medicine, Division of Nephrology, Albert Einstein College of Medicine, Bronx, NY 10461, USA. Fax: +1 718 430 8963.
*E-mail address:* victor.schuster@einstein.yu.edu (V.L. Schuster).

0006-291X/$ - see front matter © 2010 Elsevier Inc. All rights reserved.
doi:10.1016/j.bbrc.2010.03.108

well, and intracellular [$^3$H]$PGH_2$ or [$^3$H]$PGE_2$ was counted by MicroBeta scintillation counter.

To obtain the time course of $PGE_2$ transport in the presence of $PGH_2$ or TGBz T34, MDCK cells were incubated in Waymouth buffer containing 1 nM [$^3$H]$PGE_2$ at room temperature for 9 min to reach the maximum intracellular level. Thereafter, either $PGH_2$ or TGBz T34 was added to the uptake buffer at a final concentration of 2.5 or 25 μM. At the designated time, the uptake of [$^3$H]$PGE_2$ was stopped and uptake was assessed as described above. For the time course of $PGH_2$ uptake in the presence of TGBz T34, MDCK cells were incubated in Waymouth buffer containing 1 μM [$^3$H]$PGH_2$ at room temperature for 120 min to reach the maximum intracellular level. At 120 min, TGBz T34 was added to the uptake buffer at a final concentration of 25 μM. Then the transport was stopped at varied time points and uptake was quantified as above.

### 2.2. Measurements of kinetic parameters of $PGE_2$ and $PGH_2$

We repeated the time courses of $PGE_2$ or $PGH_2$ uptake in the presence or absence of 25 μM TGBz T34 at various initial extracellular concentrations of $PGE_2$ (0, 20, 40, 80, 120, 160, and 300 nM) or $PGH_2$ (0, 10, 25, 50, 100, 250, 500, and 1000 nM). In the case of $PGE_2$, at low concentrations, the extracellular concentrations were taken as $^3$H labeled $PGE_2$, which has a specific activity of 500 μCi/mol. At high concentrations of $PGE_2$, we made a mixture of $^3$H labeled and unlabeled $PGE_2$ to a final specific activity of 25 μCi/mol.

The initial velocities at various extracellular concentrations of $PGE_2$ or $PGH_2$ were determined from the $PGE_2$ uptake in the first 2 min or the $PGH_2$ uptake in the first 3 min, in the presence or absence of TGBz T34; these were linear over the early time course of $PGE_2$ or $PGH_2$ uptake. The permeability coefficient of $PGH_2$ or $PGE_2$ influx ($P_{in}$) was obtained by linear regression fit of the initial rate in the presence of TGBz T34 versus extracellular $PGE_2$ or $PGH_2$ concentration.

We subtracted the initial velocities in the presence of TGBz T34 from those in the absence of TGBz T34. These resulted initial velocities were used to obtain $K_m$ and $V_{max}$ values by nonlinear regression fit of the initial rate versus extracellular $PGE_2$ or $PGH_2$ concentration to the Michaelis–Menten equation ($V_i = V_{max}\,[S]/([S] + K_m)$).

## 3. Results

### 3.1. Time course of $PGH_2$ uptake

The time course of $PGH_2$ uptake by MDCK cells expressing PGT is shown in Fig. 1A. The circles represent the total $PGH_2$ uptake when the cells were incubated with 1 μM [$^3$H]$PGH_2$. Squares indicate experiments in which cells were incubated with 1 μM [$^3$H]$PGH_2$ in the presence of 25 μM TGBz T34, our newly identified PGT inhibitor [15]. The line with diamonds represents $PGH_2$ total uptake minus $PGH_2$ influx when the PGT inhibitor was applied, which is equivalent to PGT-mediated uptake. The "overshoot" is characteristic of PGT [17].

Fig. 1B shows $PGH_2$ uptake by wild-type MDCK cells. The inset of Fig. 1B shows the time course of $PGH_2$ uptake by wild-type MDCK cells for the first 15 min. It is evident that $PGH_2$ influx in PGT-expressing cells plus the inhibitor TGBZ T34 (squares in Fig. 1A) is almost identical to the data of Fig. 1B; each of these represents $PGH_2$ influx by simple diffusion. Since the pattern of total $PGH_2$ uptake was similar to that of PGT-mediated uptake, we conclude that PGT mediates the majority of $PGH_2$ uptake.

### 3.2. Kinetics of $PGH_2$ uptake in comparison with $PGE_2$ uptake

To obtain detailed kinetic parameters of $PGH_2$ influx, we measured initial rates of $PGH_2$ uptake at various extracellular $PGH_2$ concentrations in the presence and absence of TGBz T34. In the presence of PGT inhibitor, the plot of the initial rates of $PGH_2$ uptake versus concentration could be fitted with a straight line (squares in Fig. 2A), indicating that this part of influx was caused by simple diffusion. We calculated the permeability coefficient of $PGH_2$ influx ($P_{in}$) by diffusion by dividing the slope of this linear line by the total cell surface. $P_{in}$ for $PGH_2$ was $(5.66 \pm 0.63) \times 10^{-6}$ cm/s (Table 1).

In the absence of TGBZ T34, the plot with circles depicts the total $PGH_2$ uptake (Fig. 2A). The PGT-mediated rates (diamonds) from Fig. 2A were obtained by subtracting the influx by diffusion (squares) from the total influx (circles). When plotted against $PGH_2$ concentration, they could be fitted by the Michaelis–Menton equation (Fig. 2A). The binding constant of $PGH_2$ to PGT, $K_m$, and the maximum velocity, $V_{max}$, are listed in Table 1. PGT-mediated transport constituted 80% of $PGH_2$ influx; the remainder was mediated by diffusion.

Using the same method, we conducted a similar investigation of the kinetics of $PGE_2$ uptake. As shown in Fig. 2B, circles depict the total $PGE_2$ uptake in the absence of TGBz T34, and squares depict the $PGE_2$ influx in the presence of TGBz T34. The plot of the latter is linear and shows the component of $PGE_2$ influx caused by diffusion. $P_{in}$ for $PGE_2$, was $(1.06 \pm 0.13) \times 10^{-6}$ cm/s (Table 1). Using the same methods as for analyzing $PGH_2$ kinetics, we generated the PGT-mediated uptake component (diamonds), which could be fitted by the Michaelis–Menton equation. The binding constant of $PGE_2$ to PGT, $K_m$, and the maximum velocity, $V_{max}$, are listed in Table 1. As opposed to the case with $PGH_2$, PGT-mediated $PGE_2$ transport was almost identical to total $PGE_2$ uptake, suggesting

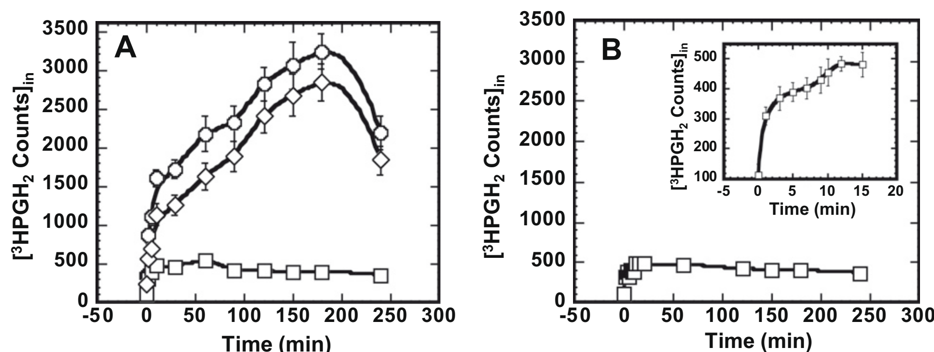


**Fig. 1.** (A) Time course of $PGH_2$ uptake by PGT-expressing MDCK cells in the presence (squares) and absence (circles) of 25 μM TGBz T34. The diamond line is formed by subtracting intracellular $PGH_2$ in the absence of TGBz T34 (circles) by intracellular $PGH_2$ in the presence of TGBz T34 (squares). (B) Time course of $PGH_2$ uptake by wild-type MDCK cells. In both (A) and (B), the values are presented as means ± SD of three individual replicates.

Download English Version:

https://daneshyari.com/en/article/1932005

Download Persian Version:

https://daneshyari.com/article/1932005

Daneshyari.com